typeset using JPSJ.sty <ver.1.0b>

Numerical Study on Aging Dynamics in the 3D Ising Spin-Glass Model. III. Cumulative Memory and 'Chaos' Effects in the Temperature-Shift Protocol

Hajime TAKAYAMA* and Koji HUKUSHIMA**

Institute for Solid State Physics, University of Tokyo, 5-1-5 Kashiwa-no-ha, Kashiwa, Chiba 277-8581

(Received February 1, 2008)

The temperature (T)-shift protcol of aging in the 3 dimensional (3D) Edwards-Anderson (EA) spin-glass (SG) model is studied through the out-of-phase component of the ac susceptibility simulated by the Monte Carlo method. For processes with a small magnitude of the T-shift, ΔT, the memory imprinted before the T-shift is preserved under the T-change and the SG short-range order continuously grows after the T-shift, which we call the cumulative memory scenario. For a negative T-shift process with a large ΔT the deviation from the cumulative memory scenario has been observed for the first time in the numerical simulation. We attribute the phenomenon to the 'chaos effect' which, we argue, is qualitatively different from the so-called rejuvenation effect observed just after the T-shift.

KEYWORDS: spin glass, slow dynamics, aging, droplet theory

§1. Introduction

Recently, in studies on slow dynamics in spin glasses,[1,2,3] the apparently contradictory phenomena, i.e., *rejuvenation* (or *chaos*) and *memory* effects in aging dynamics, have been intensively investigated.[4,5] In fact the phenomena were already observed in the early stage of study on aging in spin glasses by the so-called temperature-cycling protocol.[6] In the protocol we quench a spin glass to a temperature, say T_1, below the spin-glass (SG) transition temperature T_c from above it and let the system equilibrate (or age) for a period of t_{w1}. Subsequently, we change the temperature to T_2 ($< T_1$), age the system for a period of t_{w2}, and then the temperature is turned back to T_1. For a certain range of the parameters T_1, T_2, t_{w1} and t_{w2} some quantities such as the out-of-phase component of ac susceptibility, $\chi''(\omega;t)$, exhibit the following behavior. Just after the first T-shift $\chi''(\omega;t)$ behaves as if the system were quenched to T_2 directly from above T_c, or it looks having forgotten the aging at T_1 before the T-shift. This is called the rejuvenation (or chaos) effect. However, after the temperature is turned back to T_1, $\chi''(\omega;t)$ observed is the one we expect as a simple extension of $\chi''(\omega;t)$ already aged by t_{w1} at T_1. Thus the system definitely preserves the memory of the previous aging at T_1, while it apparently exhibits the rejuvenation behavior, in the aging process at T_2. The proper understanding of such a peculiar phenomenon is believed to shed light not only on the mechanism behind the aging dynamics but also the nature of the SG phase itself. Furthermore it will provide us with powerful concepts to understand the glassy dynamics in various related systems such as orientational glasses,[7] polymers,[8] and interacting nanoparticles systems.[9]

By the real-space interpretation, or by the droplet picture,[10,11,12] which we have been adopting in our recent studies,[13,14,15,16] the SG order is considered to grow up slowly in aging processes. In particular, we have demonstrated that the SG coherence length, which we regards as the mean size of SG domains developed in aging, continuously grows even under the T-shift process.[15] This we call the *cumulative memory* effect. We have further extended this characteristics to a scenario that the SG short-range order ever grows continuously with growth rates sensitively dependent on the temperature so long as the system is in the SG phase.[16] Let us call this the *cumulative memory scenario*, and denote the mean size of SG domains as $R_{T[t]}(t)$, where $T[t]$ symbolically represents the temperature changes that the system has experienced up to time t from the first quench to the SG phase at $t = 0$. It has been demonstrated that the time evolution of zero-field-cooled (ZFC) magnetizations observed in various schedules of temperature changes but with a common initial quench condition[17] are well described by a unique function of $R_{T[t]}(t)$.[16]

The purpose of the present work is to numerically explore to what extent the simulated data of $\chi''(\omega;t)$ in the T-shift protocol of the 3D Ising EA SG model are compatible or incompatible with the cumulative memory scenario, and with the rejuvenation (chaos) and memory effects mentioned above. For this purpose we certainly need a few more length and time scales than $R_{T[t]}(t)$. One is $R_{T[t]}(t)$ at $t = t_{w1}$, i.e., the mean domain size grown in the isothermal aging after quench to the SG phase, which is denoted as $R_{T_1}(t_{w1})$. After the temperature is shifted to T_2 spin configurations within each domains, which were in local equilibrium of T_1 just before the T-shift, gradually become in local equilibrium of T_2.

* E-mail: takayama@issp.u-tokyo.ac.jp
** E-mail: hukusima@issp.u-tokyo.ac.jp

By the word 'gradually' we mean that the change associates with slowly growing droplets (or subdomains) of a mean size $L_{T_2}(\tau)$ ($< R_{T_1}(t_{\rm w1})$) with $\tau = t - t_{\rm w1}$. Here we call this the *droplets-in-domain* scenario (previously called the *quasi-domains-within-domains* picture[15]) .

A key quantity of the present work is the time scale required for $L_{T_2}(\tau)$ to catch up $R_{T_1}(t_{\rm w1})$.[15] At time scales larger than this one, denoted as $t_{\rm w1}^{\rm eff}$, behavior of physical quantities such as $\chi''(\omega;t)$ cannot be distinguished, within the accuracy of measurement, from the corresponding behavior in the isothermal aging at T_2. In other words, the system merges to a T_2-isothermal aging state at the time scale of $t_{\rm w1}^{\rm eff}$ after the T-shift. The latter is regarded as the *effective waiting time* of the $t_{\rm w1}$-aging at T_1 reread as an T_2-isothermal aging. If the cumulative memory scenario holds, $t_{\rm w1}^{\rm eff}$ is the time required for the SG coherence to grow in the T_2-isothermal aging up to $R_{T_1}(t_{\rm w1})$, i.e.,

$$L_{T_2}(t_{\rm w1}^{\rm eff}) = R_{T_2}(t_{\rm w1}^{\rm eff}) = R_{T_1}(t_{\rm w1}). \tag{1.1}$$

is expected to hold. Here the first equality simply indicates that $L_T(t)$ has the same functional form as that of $R_T(t)$ since the both growth processes are governed by common thermally-activated dynamics.

In the present work we have extensively examined T-shift processes in the 3D Gaussian EA model with $T_{\rm c} \simeq 0.95J$[18] through the ac susceptibility $\chi''(\omega;t)$ simulated by the standard Monte Carlo (MC) simulation. Here J is the variance of the interactions. The temperature range investigated is $T \sim [0.4, 0.7]$ in unit of J, and the time range is up to 10^5 MC steps. One of the results we have found is that in negative (positive) T-shift protocols with $T_1 \to (\leftarrow)\ T_2$ Eq.(1.1) (the same equation but with the suffix 1, 2 interchanged) holds well when $\Delta T = T_1 - T_2 = 0.1$. This confirms the cumulative nature of aging in both negative and positive T-shift protocols with a small ΔT. A more interesting result is that, for the negative T-process with $T_1 = 0.7, T_2 = 0.4$ significant violation of Eq.(1.1) has been observed, while in the corresponding positive T-shift protocol Eq.(1.1) is satisfied within accuracy of the present numerical analysis. The former non-cumulative memory effect has been, for the first time to our knowledge, observed in simulations on the 3D EA models. Although the phenomena appear asymmetrically with respect to the direction of temperature changes, the deviation from the cumulative memory scenario in the negative T-shift appears qualitatively similarly to the one observed recently in experiments on the AgMn spin glass.[19] We tentatively regard them as an effect associated with the temperature-chaos effect in the equilibrium SG phase,[10,11] and call them the *'chaos effect'*. In contrary, as in the previous work,[20,21] such rejuvenation effects observed experimentally just after the T-shift have not been detected even with $\Delta T = 0.3$ in the present work.

The organization of the paper is as follows. In the next section we describe our strategy of the simulation and the method to evaluate $\chi''(\omega;t)$ from the spin autocorrelation function making use of the fluctuation-dissipation theorem. In §3 we explain how to specify the effective waiting time $t_{\rm w1}^{\rm eff}$ from the obtained data of $\chi''(\omega;t)$, and present the results of $t_{\rm w1}^{\rm eff}$, or $R_{T_2}(t_{\rm w1}^{\rm eff})$ for T-shift processes with various sets of T_1 and T_2. In the final section we discuss our results, emphasizing on the length and time scales involved as well as on the relation to the experimental results.

§2. Method of Analysis

Numerical simulation on a well-defined microscopic SG model, such as the EA model investigated in the present work, is of quite importance in studying aging phenomena. It enables us to faithfully realize any T-shift process and observe any quantity in principle. For example, the SG coherence length $\xi_{T[t]}(t)$, which we regard as the mean SG domain size $R_{T[t]}(t)$, has been calculated from the replica overlap function.[15] For the isothermal process of the 3D Ising Gaussian EA model which we study in the present work, it is well described by the power law[15,22,23] written as

$$R_T(t)/l_0 = b_T(t/t_0)^{1/z(T)}, \tag{2.1}$$

where l_0 and t_0 are microscopic length and time scales ($l_0 = 1$ lattice distance and $t_0 = 1$ MC step for simulated results), b_T is a weakly T-dependent constant, and the exponent $1/z(T)$ linearly depends on T except for the region near $T_{\rm c}$.[13]

The growth law of $R_T(t)$ in isothermal aging different from Eq.(2.1) was proposed in the droplet theory due to Fisher and Huse.[12] It is written as[24]

$$R_T(t)/L_0(T) = \tilde{L}(t/\tau_0(T)), \tag{2.2}$$

with the scaling function $\tilde{L}(x)$ given by

$$\tilde{L}(x) \sim \begin{cases} x^{1/z} & (x \ll 1), \\ \log^{1/\psi}(x) & (x \gg 1). \end{cases} \tag{2.3}$$

Here $L_0(T)$ ($\sim l_0\epsilon^{-\nu}$) is the crossover length, $\tau_0(T)$ ($\sim t_0\epsilon^{-z\nu}$) is the attempt time for thermal activation process of droplets, where $\epsilon = (T_{\rm c} - T)/T_{\rm c}$, and z and ν are the critical exponents associated with the criticality at $T_{\rm c}$. The exponent ψ in Eq.(2.3) is, on the other hand, intrinsic to the activation dynamics of droplets. We have recently confirmed the above growth law, including the crossover from the critical dynamics ($x \ll 1$) to the activated dynamics ($x \ll 1$), in the EA SG model but in 4 dimension[24] (see also[21]). However, the simulated data of $R_T(t)$ in the 3D EA model are compatible with both the power law of Eq.(2.1) and the logarithmic law in Eq.(2.3).[21,22]

Our strategy in the present work is as follows. Because of the circumstances of the 3D EA model mentioned just above as well as those of the recent experiment,[25] we do not go into the question which growth law is a correct one for $R_T(t)$ observed in the time-window ($\lesssim 10^5$ MCS) of the simulations, and simply use our results, i.e., Eq.(2.1), in relating a time scale of observation to a length scale of the SG short-range order. Then we examine whether the cumulative memory scenario is sufficient or not to interpret the obtained results of the length scales. We also restrict ourselves to the temperature range of $T/J = [0.4, 0.7]$ as already noted in §1. In

this temperature range $1/z(T)$ in Eq.(2.1) is well proportional to T and the dynamics is considered to be dominated by the activated process. But the prefactor b_T still exhibits weak dependence on T even in this range which will turn out not to be neglected in our present analysis. Lastly we have examined T-shift processes with various values of the temperature differences ΔT, in particular, a larger one than that studied in our previous work.[15)]

In the aging study at T through the ac susceptibility at frequency ω we need to introduce another length scale, $L_T(t_\omega)$, with $t_\omega = 2\pi/\omega$. It is a mean size of spin clusters (or droplets) which can respond to the ac field at T. In the droplet picture the aging (or t-dependent) part of $\chi''(\omega;t)$ in an isothermal aging is described by a function of $L_T(t_\omega)/R_T(t)$.[12,14)] As will be discussed in §4 below, $\chi''(\omega;t)$ in some T-shift process to T at $t = t_{\rm w}$ is given in terms of $L_T(t_\omega)/L_T(\tau)$ where $\tau = t - t_{\rm w}$. Thus it provides us information of $R_T(t)$ or $L_T(\tau)$ in the aging process since $L_T(t_\omega)$ is independent of t or τ.

By the experimental condition of measuring $\chi''(\omega;t)$, t or τ is necessarily larger than t_ω in general. This time regime is called the quasi-equilibrium one, where the fluctuation-dissipation theorem (FDT) is expected to hold well, though approximately.[26,27)] Therefore, in the present work, the out-of phase component of ac susceptibility, $\chi''(\omega;t)$, is evaluated from the spin autocorrelation function

$$C(\tau;t) = \overline{\langle S_i(\tau+t)S_i(t)\rangle}, \tag{2.4}$$

via the FDT as[14)]

$$\chi''(\omega;t) \simeq -\frac{\pi}{2T}\frac{\partial}{\partial \ln\tau}C(\tau;t)\Big|_{\tau=t_\omega}. \tag{2.5}$$

In Eq.(2.4), $S_i(t)$ is the sign of the Ising spin at site i at time t which is measured in unit of one MC step. The over-line denotes the averages over sites and over different realizations of interactions (samples), and the bracket the average over thermal noises (or different MC runs). In this evaluation of $\chi''(\omega;t)$ we are completely free from any nonlinear effect of the ac-field amplitude.[20)]

In our previous work[15)] we studied the susceptibility defined by

$$\tilde{\chi}(\omega;t) = \frac{1}{T}[1 - C(\tau;t)]\Big|_{\tau=t_\omega}. \tag{2.6}$$

It is just the ZFC susceptibility: the induced magnetization (divided by h) at an elapsed time of τ under the field h which is switched on after the system has aged under $h = 0$ by a period of t. For slow processes of our present interest, $\tilde{\chi}(\omega;t)$ is essentially regarded as the in-phase component of the ac susceptibility, $\chi'(\omega;t)$. As in the experiments, simulated $\chi''(\omega;t)$ exhibits larger effects of aging relatively to its own absolute magnitude than $\chi'(\omega;t)$ or $\tilde{\chi}(\omega;t)$ does. However we have to numerically evaluate the logarithmic derivative in Eq.(2.5) to estimate $\chi''(\omega;t)$. In the present work we have calculated several $C(\tau;t)$ in Eq.(2.4), each of which is the average over one MC run for each sample but typically over 1600 samples. The linear system size is fixed to $L = 24$. The error bars on $\chi''(\omega;t)$ drawn in the figures shown below indicate the variance in the results of the numerical derivative on these several sets of $C(\tau;t)$.

§3. Results

3.1 Isothermal aging

Before going into discussions on the T-shift protocol, let us here present the results of $\chi''(\omega;t)$ obtained in the isothermal aging. In Fig. 1 we show $\chi''(\omega;t)$ with $t_\omega = 64$ in the isothermal aging at various temperatures. They play an important role in the following arguments on the T-shift protocol, and we call them the *reference curve* at each temperature.

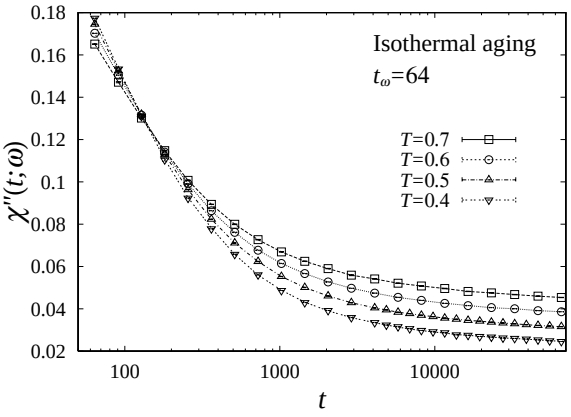

Fig. 1. $\chi''(\omega;t)$ with $t_\omega = 64$ in the isothermal aging at various temperatures.

In Fig 2 $\chi''(\omega;t)$ at $T = 0.6$ for $t_\omega = 16 \sim 256$ are shown. The filled symbols are raw data plotted directly against t, while the open symbols are the same $\chi''(\omega;t)$ plotted against ωt with no vertical shifts of the data sets. All the sets of data thus plotted nicely collapse to a universal curve. This reconfirms that the ωt-scaling of $\chi''(\omega;t)$ holds also in the present model spin glass[20)] as observed experimentally.[1)] As pointed out in §2, the time evolution of $\chi''(\omega;t)$ is considered to be a function of $L_T(t_\omega)/R_T(t)$ in the droplet picture. The ωt-scaling then comes out from the first equality of Eqs.(1.1) and (2.1).[14)] The response in equilibrium, $\chi''_{\rm eq}(\omega) = \lim_{t\to\infty}\chi''(\omega;t)$, is hardly extracted from our present data. We could not detect even its relative difference with ω, which should be reflected as the vertical shifts of the data sets in the above scaling analysis.

3.2 T-shift protocol

In Fig. 3 we show $\chi''(\omega;t)$ with $t_\omega = 64$ numerically observed in the *negative (positive)* T-shift protocol. The temperature is changed from $T_1 = 0.7$ ($T_2 = 0.5$) to $T_2 = 0.5$ ($T_1 = 0.7$) at different waiting times $t_{\rm w1}$ ($t_{\rm w2}$). The observation starts from $t = t_{\rm wi} + t_\omega$ after each T-shift. Similarly to $\tilde{\chi}(\omega;t)$ previously investigated,[15)] we see the following characteristic features.

a) Each $\chi''(\omega;t)$ rapidly undershoots (overshoots) the T_2 (T_1)-reference curve.

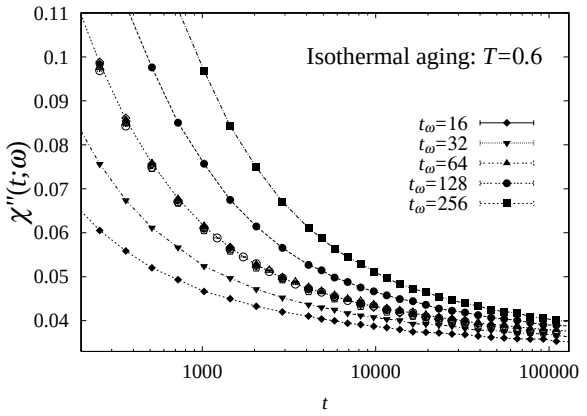

Fig. 2. $\chi''(\omega;t)$ in the isothermal aging at $T = 0.6$. The filled symbols are the data plotted directly against t, while the open symbols are the same data plotted against $64t/t_\omega$.

b) $\chi''(\omega;t)$ merges to the T_2 (T_1)-reference curve from below (above).

For the negative T-shift, in particular, the value of $\chi''(\omega;t)$ just after the negative T-shift is the larger relatively to the T_2-reference curve, the larger is $t_{\rm w1}$. However, $\chi''(\omega;t)$ just after the shift does not exhibit overshooting of the T_1-reference curve, a phenomenon which we call the *strong rejuvenation* effect in the present paper. This is also the case even if we dare to measure $\chi''(\omega;t)$ at $\tau = t - t_{\rm w1}$ smaller than t_ω.[21)]

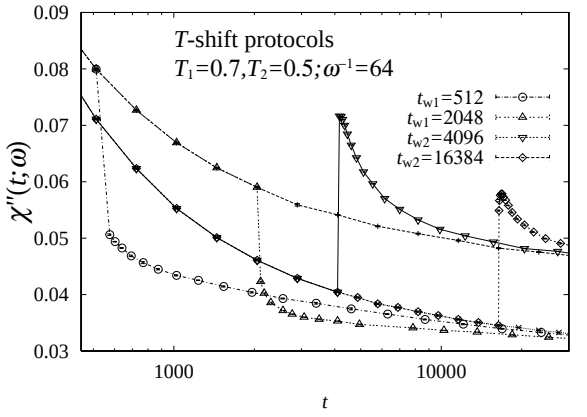

Fig. 3. $\chi''(\omega;t)$ in aging with negative and positive T-shifts between $T_1 = 0.7$ and $T_2 = 0.5$ at $t = t_{{\rm w}i}$ indicated in the figure. The upper and lower curves with the smaller symbols represent the T_1- and T_2-reference (isothermal) curves, respectively.

3.3 Effective waiting time

Feature b) above is examined in more details in Figs. 4 and 5. We note that the t-axis in these figures is linear in t. Within the time window of Fig. 4 the merging of bare $\chi''(\omega;t)$ (denoted by $t_{\rm sh1} = 0$) to the T_2-reference curve is not seen. If, however, the branch of $\chi''(\omega;t)$ at $t > t_{\rm w1}$ is shifted to the *right* by an amount denoted by $t_{\rm sh1}$, it crosses the reference curve and merges to it at a smaller t than that with $t_{\rm sh1} = 0$. At a certain value of $t_{\rm sh1}$ ($\simeq 3300 - 512$ in the figure) it merges to the reference curve and lies on it afterwards. We regard time τ required for the shifted branch to merge to the reference curve in this situation as the effective waiting time, $t_{\rm w1}^{\rm eff}$, introduced in §1. If $t_{\rm sh1}$ is further increased the branch merges to the reference curve from above and again at larger t than $t_{\rm w1}^{\rm eff}$. Thus the chosen $t_{\rm sh1}$ which corresponds to $t_{\rm w1}^{\rm eff}$ yields the shortest time for the shifted branch to merge to the reference curve.

An interesting observation in the above analysis is that the time at which the properly shifted branch merges to the T_2-reference curve is nearly equal to $2t_{\rm w1}^{\rm eff}$; $t_{\rm w1} + t_{\rm sh1} + t_{\rm w1}^{\rm eff} \simeq 2t_{\rm w1}^{\rm eff}$ and so $t_{\rm w1}^{\rm eff} \simeq t_{\rm w1} + t_{\rm sh1}$. This aspect, which is by no means trivial, has been commonly observed in most of the T-shifts examined in the present work. Using this observation, we estimate errors of $t_{\rm w1}^{\rm eff}$ as follows. We judge by eyes the largest $t_{\rm sh1}$ for which the shifted branch of $\chi''(\omega;t)$ certainly crosses with but not merges to the reference curve, and this value of $t_{\rm sh1}$ gives a smallest estimate of $t_{\rm w1}^{\rm eff}$. Similarly the smallest $t_{\rm sh1}$ for which the shifted branch merges to the reference curve at $t \gtrsim 3t_{\rm w1}^{\rm eff}$ yields a largest estimate of $t_{\rm w1}^{\rm eff}$. The three shifted branches shown in Fig. 4 correspond to these smallest, mean, and largest estimates for $t_{\rm w1}^{\rm eff}$.

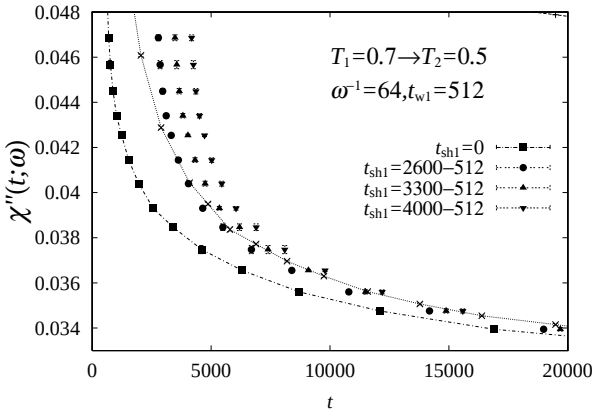

Fig. 4. $\chi''(\omega;t)$ in the negative T-shift protocol from $T_1 = 0.7$ to $T_2 = 0.5$. Each symbol represents the branch of $\chi''(\omega;t)$ at $t > t_{\rm w1}$ shifted by an amount of $t_{\rm sh1}$ indicated in the figure. the line with the smaller symbols is the T_2-reference curve.

The above analysis for the negative T-shift protocol also works for the positive T-shift protocol. A typical example from $T_2 = 0.5$ to $T_1 = 0.7$ with $t_{\rm w2} = 16384$ is shown in Fig. 5, for which we have to reread the suffix 1 by 2 and vice versa in the above argument. Also in this case the branch of $\chi''(\omega;t)$ at $t > t_{\rm w2}$ is shifted to the *left* by $t_{\rm sh2}$. A too large $t_{\rm sh2}$ makes the shifted branch to overshoot the T_1-reference curve, while a too small $t_{\rm sh2}$ significantly delays the merging. With a proper chosen $t_{\rm sh2}$ we obtain $t_{\rm w2}^{\rm eff}$ ($\simeq 1600$ from the figure) which satisfies $t_{\rm w2}^{\rm eff} = t_{\rm w2} - t_{\rm sh2}$. Its error bar is similarly evaluated from the two other $t_{\rm sh2}$'s indicated in the figure.

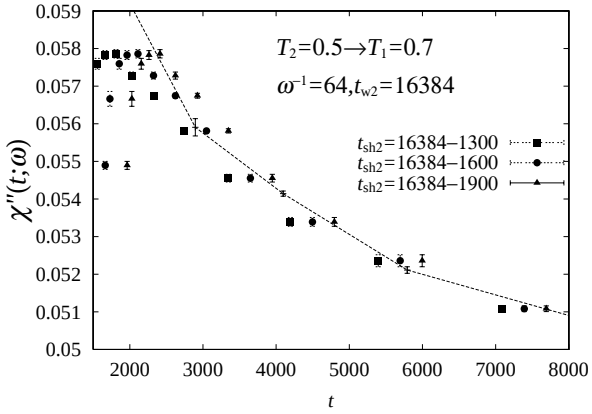

Fig. 5. $\chi''(\omega;t)$ with $t_\omega = 64$ in the positive T-shift protocol from $T_2 = 0.5$ to $T_1 = 0.7$ with $t_{w2} = 16384$. The data in a large time scale are shown in Fig. 3. The three sets of symbols represent the branches of $\chi''(\omega;t)$ at $t > t_{w2}$ shifted to the left by the amount t_{sh2} indicated in the figure. The line is the T_1-reference curve.

3.4 Cumulative memory and 'chaos' effects

In Fig. 6 we plot $t_{w1}^{\rm eff}$ (t_{w2}) as a function of t_{w1} ($t_{w2}^{\rm eff}$) obtained in the previous subsection in the negative (positive) T-shift protocol for three sets of (T_1, T_2). Here we have followed the idea of 'twin-experiments' in the recent work.[19] Before the explanation of the lines drawn in the figure, we note that the data points of both negative and positive T-shifts with $T_1 = 0.7$, $T_2 = 0.6$ are seen to lie on a certain common curve, while this is not the case for those with $T_1 = 0.7$ and $T_2 = 0.4$. The former is expected from the cumulative memory scenario. But the latter data points clearly indicate a violation to the scenario irrespectively of the growth law of the SG domains.

Now let us explain the lines in Fig. 6. The solid ones represent the relation between the $t_{w1}^{\rm eff}$ (t_{w2}) and t_{w1} ($t_{w2}^{\rm eff}$) when the cumulative memory scenario represented by Eq.(1.1) (the one whose suffix 1, 2 interchanged) combined with the growth law of Eq.(2.1) holds. For the latter we have explicitly used the following sets of the parameter values $(T; z(T), b_T)$ we previously obtained:[13] (0.7; 8.71, 0.779), (0.6; 9.84, 0.782), (0.5; 11.76, 0.800) and (0.4; 14.80, 0.818). As seen in the figure, for a small ΔT (= 0.1), both $t_{w1}^{\rm eff}$ and $t_{w2}^{\rm eff}$ lie on the solid line. The results confirm the cumulative memory scenario described in §1. With $\Delta T = 0.2$, $t_{w2}^{\rm eff}$ still lie on the solid line but $t_{w1}^{\rm eff}$ tends to deviate, though a little, from it. For $\Delta T = 0.3$, $t_{w1}^{\rm eff}$ significantly deviate from the solid line, which is incompatible with the cumulative memory scenario. It should be emphasized, however, that the corresponding $\chi''(\omega;t)$ (not shown) in this process exhibit features a), b) mentioned in §3.2, i.e., no strong rejuvenation.

If the weak T-dependence of b_T is discarded the condition of Eq.(1.1) is reduced to

$$\left(\frac{t_{w1}^{\rm eff}}{\tau_0}\right) = \left(\frac{t_{w1}}{\tau_0}\right)^{T_1/T_2}, \qquad (3.1)$$

which is also shown by the dotted lines in Fig. 6. For $\Delta T = 0.1$ the effect of the T-dependence of b_T is negligibly small. The effect is, however, significant for $\Delta T \geq 0.2$. Thus the T-dependence of b_T has to be properly taken into account to judge the cumulative nature of memory observed even in the temperature range examined in the present simulation.

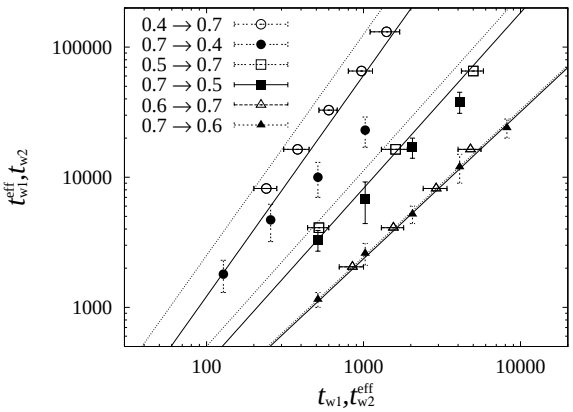

Fig. 6. $t_{wi}^{\rm eff}$ vs t_{wi} for the negative ($i = 1$) and positive ($i = 2$) T-shift protocols for three sets of T_1 and T_2 indicated in the figure. The lines represent the expected behavior from Eqs.(1.1) and (2.1) as explained in the text.

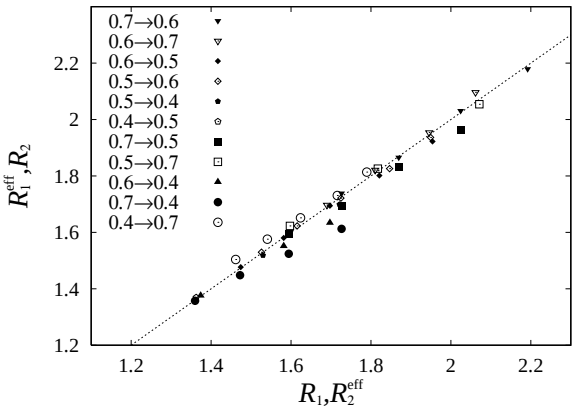

Fig. 7. Relations $t_{wi}^{\rm eff}$ vs. t_{wi} drawn by means of the corresponding domain sizes evaluated by Eq.(1.1) with Eq.(2.1). Here we omit the error bars. For all the sets of T_1, T_2 their magnitudes are comparable with those shown in Fig. 6.

In Fig. 7 we replot our data in Fig. 6 as well as those of other sets of (T_1, T_2) in terms of the lengths, where $R_1 \equiv R_{T_1}(t_{w1})$ and $R_1^{\rm eff} \equiv R_{T_2}(t_{w1}^{\rm eff})$ which are evaluated by Eq.(2.1) using t_{w1} and $t_{w1}^{\rm eff}$ extracted in the negative T-shift processes (R_2 and $R_2^{\rm eff}$ in the positive T-shift process are similarly evaluated). The line in the figure is what is expected from the cumulative memory scenario, i.e., $R_i^{\rm eff} = R_i$ for both $i = 1, 2$. We see clearly that this is the case for both negative and positive T-shift processes with $\Delta T = 0.1$ within the time window of the present simulation. For $\Delta T = 0.2$ the data of the positive T-shift satisfy the condition $R_2^{\rm eff} = R_2$, but those of the negative T-shift exhibit the tendency $R_1^{\rm eff} < R_1$.

Behavior of the T-shift with $\Delta T = 0.3$, i.e., $T_1 = 0.7$ and $T_2 = 0.4$ is as already described above and is interpreted below to be due to the 'chaos effect.'

According to the theory for the temperature-chaos in spin glasses,[11,10] the SG equilibrium configurations at different temperatures, T_1 and T_2, are completely uncorrelated with each other in the length scale larger than $l_{\Delta T} \propto \Delta T^{-1/\zeta}$, where $l_{\Delta T}$ is called the overlap length and ζ (> 0) the chaos exponent. An important problem here is how the existence of $l_{\Delta T}$ affects the non-equilibrium aging dynamics. Let us consider a negative T-shift process with ΔT, for which $l_{\Delta T}$ is supposed to be sufficiently smaller than $R_{T_1}(t_{\rm w1})$, and introduce the time scale $t_{\rm ov1}$ by $L_{T_2}(t_{\rm ov1}) = l_{\Delta T}$. At a time range after the T-shift specified as $t_{\rm w1}^{\rm eff} \gg \tau \gg t_{\rm ov1}$, a longer part of the memory imprinted before the T-shift is still preserved, but such a memory is expected to be irrelevant to the equilibration process to the SG ordered state at $T = T_2$. Thus the system looks as if it is already in the isothermal aging state at T_2. Then, if our analysis to determine $t_{\rm w1}^{\rm eff}$ is applied to this T-shift process, the expected result is $t_{\rm w1}^{\rm eff} \simeq t_{\rm ov1}$ irrespectively of $t_{\rm w1}$. The circumstances are the same for the positive T-shift protocol. Consequently, $R_i^{\rm eff}$ in Fig. 7 is expected to saturate to $l_{\Delta T}$ at large R_i both for $i = 1, 2$, and the data for the negative and positive T-shifts come out symmetrically with respect to the line of $R_i^{\rm eff} = R_i$.

We tentatively interpret our data of the negative T-shift with $\Delta T = 0.3$ as an early stage of the saturation described above. Unfortunately, the data are so limited that we cannot figure out a value of $l_{\Delta T}$. Also the corresponding positive T-shift data nearly coincide with the line $R_i^{\rm eff} = R_i$, i.e., the two sets of data are by no means symmetric with respect to the line. One of the reason of this asymmetric behavior may be due to our method to specify the effective aging time combined with the time scales in our simulation. Although $l_{\Delta T}$ is common to the negative and positive T-shifts, the separation of time scales $t_{\rm w2}, t_{\rm ov2}$ and $t_{\rm w2}^{\rm eff}$ in the positive T-shift is much smaller than that of $t_{\rm w1}, t_{\rm ov1}$ and $t_{\rm w1}^{\rm eff}$ in the negative T-shift. This is due to a large difference in the growth rates at the two temperatures. It is then rather hard to detect a possible small difference between $t_{\rm ov2}$ and $t_{\rm w2}^{\rm eff}$ within our present analysis. With these reservations, we interpret our results of the T-shift process with $\Delta T = 0.3$ as a dynamic process which reflects the temperature-chaos predicted for the equilibrium SG phase.

§4. Discussions

In the T-shift protocol examined in the present study, the cumulative memory scenario has been confirmed for T-shift processes with a small magnitude of the shift, i.e., $\Delta T = T_1 - T_2 = 0.1$. This has been done by close comparisons of $\chi''(\omega; t)$ after the T-shift with that in the isothermal aging at T_2 (reference curve). However, there have been little experiments which directly measure $t_{\rm w1}^{\rm eff}$ similarly to our analysis.[28,29] An example is the one by Mamiya *et al*,[28] who analyzed the aging dynamics in the SG-like phase of a ferromagnetic fine particles system. In the T-shift process with $T_1 = 49$K and $T_2 = 47$K (with $T_{\rm g} \simeq 70$K) they observed $t_{\rm w1}^{\rm eff} \sim 3 \times t_{\rm w1}$ for $t_{\rm w1} = 2.0, ..., 15.0$ks. If we suppose $\tau_0 = 10^{-6}$s for a magnetic moment carried on by each fine particle,[30] we obtain $t_{\rm w1}^{\rm eff} \simeq (2.4 \sim 2.7) \times t_{\rm w1}$ from Eq.(3.1). The result is rather satisfactory and implies that the cumulative memory scenario works as well for the T-shift process with a small ΔT in this SG material.

Our results on the negative T-shift protocol with $\Delta T = 0.3$ have turned out to be incompatible with the cumulative memory scenario. The period $t_{\rm w1}^{\rm eff}$ necessary for the system to become in a T_2-isothermal aging state after the T-shift is significantly smaller than the value of $t_{\rm w1}^{\rm eff}$ estimated from Eq.(1.1) combined with Eq.(2.1). In this negative T-shift process which violates the cumulative memory scenario, however, the strong rejuvenation phenomenon just after the T-shift, which is described in §3.2, has not been detected. We have therefore attributed the non-cumulative memory effect we have found to the 'chaos effect'.

Quite recently Jönsson *et al.* (JYN) have reported the chaos effect which symmetrically appears in the positive and negative T-shifts in a Heisenberg-like spin glass AgMn.[19] They have measured the ZFC magnetization with schedules of temperature change corresponding to the T-shift protocol discussed in the present work but within a very small range of ΔT ($\leq 0.012 T_{\rm c}$). The logarithmic-time derivative of the ZFC magnetization, $S(t; t_{\rm w1})$, exhibits a peak, whose position is considered to be at $\tau = t - t_{\rm w1} \simeq t_{\rm w1}^{\rm eff}$, the time required for the merging to an isothermal state at the new temperature just investigated in the present work (see the discussion below). In fact, our $R_1^{\rm eff}$-vs-R_1 plot in Fig. 7 of the negative T-shift with $\Delta T = 0.3$ is in qualitative agreement with their $L_{\rm eff}$-vs-$L_{T_i}(t_{\rm w})$ plot, where their $L_{\rm eff}$ ($L_{T_1}(t_{\rm w})$) just corresponds to our $R_1^{\rm eff}$ (R_1). In contrast to our numerical observation, however, their data for the positive T-shift plotted in our way appear symmetrically to the negative one with respect to the line $R_i^{\rm eff} = R_i$. The overlap length $l_{\Delta T}$ estimated by scaling analysis has turned out to be larger than R_i ($= L_{T_i}(t_{\rm w})$), or before the saturation of $R_i^{\rm eff}$ mentioned in §3.4. One of the reasons of this discrepancy between their experiment and our simulation may be the Heisenberg-spin nature in their material AgMn; Heisenberg spin glasses are more chaotic than Ising spin glasses.[19,31] This point is very interesting and to be further pursued.

Next let us make a few comments on aging at a time range $\tau = t - t_{\rm w1} \lesssim t_{\rm w1}^{\rm eff}$ after the T-shift, which we have called the transient regime of the T-shift process.[15] A main idea for this regime is the droplets-in-domain scenario which involves at least two characteristic length scales as mentioned in § 1. One is the mean domain size at $\tau = 0$, i.e., $R_{T_1}(t_{\rm w1})$ and the other is $L_{T_2}(\tau)$, the mean size of droplets (or subdomains) which are already in local equilibrium of the shifted temperature T_2 at time τ after the T-shift. Associated with the growth of $L_{T_2}(\tau)$ some peculiar features have been observed. An example is a non-monotonic time evolution of the energy density in a positive T-shift process (see Fig. 4 in[15]). It is recently named as the Kovacs effect in[21] since the qualitatively similar phenomenon was first observed in polymer glasses.[32]

In the droplets-in-domain scenario here we implicitly assume that droplets (or subdomains) in local equilibrium of T_2 distinguish themselves from those in local equilibrium of T_1. On the other hand, the Kovacs effect has been observed in negative T-shift processes with $\Delta T = 0.2$, for which the 'chaos effect' is not clearly detected in Fig. 7, or $l_{\Delta T} > R_{T_1}(t_{\rm w1})$. This strongly suggests that in nonequilibrium aging dynamics the spin configurations which we have so far supposed to be in local equilibrium at two different temperatures differ from each other even in length scales shorter than the equilibrium $l_{\Delta T}$ of the corresponding temperatures. This viewpoint is in contrast to the argument of the temperature-chaos in equilibrium, and is worthy to be investigated.

From the droplets-in-domain scenario mentioned just above, the strong rejuvenation experimentally observed in the ac susceptibility measurement discussed in §3.2 can be regarded as one of such peculiar phenomena in the transient regime. As mentioned in §2, the ac response associates another short length scale $L_{T_2}(t_\omega)$. In the time range $t_\omega \ll \tau \ll t_{\rm w1}^{\rm eff}$ so that $L_{T_2}(t_\omega) < L_{T_2}(\tau) < R_{T_1}(t_{\rm w1})$ holds, the t-dependent part of $\chi''(\omega;t)$ is governed dominantly by the ratio $L_{T_2}(t_\omega)/L_{T_2}(\tau)$ since droplets responding to the ac field less feel the existence of larger domains of $R_{T_1}(t_{\rm w1})$ than that of smaller subdomains of $L_{T_2}(\tau)$. The strong rejuvenation alone is therefore not necessarily incompatible with the cumulative memory scenario. In neither the previous[15,20,21] nor the present simulations, however, the strong rejuvenation has been detected. This may be again attributed to the smallness of the time window; the separation of the time scales, $t_\omega \ll \tau \ll t_{\rm w1}^{\rm eff}$, is not enough in the simulations.

Quite recently Yoshino and the present authors have argued based on the numerical results on the 4D Ising EA model that fluctuations of droplets, whose size becomes comparable to that of the preexisting domains, become anomalously large, and that they are responsible to the occurrence of a peak in $S(t;t_{\rm w})$ of the isothermal ZFC magnetization at $\tau \simeq t_{\rm w}$ where $\tau = t - t_{\rm w}$ is the time elapsed after the measuring field is applied.[24] At the end of the transient regime of the T-shift process, or at the merging to a T_2-isothermal aging state, similar large fluctuations and so a peak in $S(t;t_{\rm w1})$ at $\tau \simeq t_{\rm w1}^{\rm eff}$ are expected to appear so long as ΔT is relatively small. In fact this has been experimentally observed[19] as already mentioned above.

Combining the arguments based on our numerical results, in particular, the droplets-in-domain scenario and the cumulative memory one, with a possible existence of the 'chaos effect', we can think of the following behavior that a spin glass exhibits in the negative T-shift protocol of aging depending on the magnitude of ΔT (and similar behavior also for the positive T-shift protocol). For a sufficiently small ΔT, the merging to the T_2-isothermal aging state is observed at $\tau \simeq t_{\rm w1}^{\rm eff}$, where $t_{\rm w1}^{\rm eff}$ is given by Eq.(1.1), i.e., by the cumulative memory scenario. When ΔT becomes large, both the strong rejuvenation just after the T-shift and the merging to the T_2-isothermal aging state at $\tau \simeq t_{\rm w1}^{\rm eff}$ are expected to be observed. The latter, however, becomes to be hardly detected by such an ac susceptibility analysis done in the present work since $L_{T_2}(t_\omega)$ is much smaller than $L_{T_2}(t_{\rm w1}^{\rm eff})$. Instead, it is observed through a peak in $S(t;t_{\rm w1})$ of the ZFC magnetization.[33] The extracted value of $t_{\rm w1}^{\rm eff}$ in this case either satisfies the cumulative memory scenario ($t_{\rm ov1} \gg t_{\rm w1}^{\rm eff}$) or is already strongly affected by the chaos effect ($t_{\rm ov1} \sim t_{\rm w1}^{\rm eff}$).

What is the expected behavior for T-shift processes with a sufficiently large ΔT for which $t_{\rm ov1} \ll t_{\rm w1}^{\rm eff}$ or even $t_{\rm ov1} \ll t_{\rm min}^{\rm obs}$ holds? Here $t_{\rm min}^{\rm obs}$ is the shortest time that the temperature T_2 is experimentally stabilized after the T-shift. The recent experimental results are claimed to reach this regime,[19,33] and a theory for the chaos effect on T-shift and T-cycling processes in this regime has been proposed by Yoshino *et al.*[34] Unfortunately this regime has not been realized in the numerical simulations on the 3D EA model. Probably it needs a sufficiently large $t_{\rm w1}$, larger than the time-window of our simulation ($\lesssim 10^5 t_0$), to realize the condition $R_{T_1}(t_{\rm w1}) > l_{\Delta T}$. In order to further explore aging dynamics in the T-shift protocol, one has to systematically choose values of the parameters ΔT and $t_{{\rm w}i}$ even in experiments, since their time-window is similarly small (~ 5 decades) to that of the numerical simulation though its absolute magnitude is large ($1s \sim 10^{12} t_0$).

To conclude, we have numerically studied the T-shift protocol of aging in the 3D EA spin-glass model through the measurement of the ac susceptibility. For processes with a small magnitude of the T-shift, ΔT, the memory imprinted in the first stage of isothermal aging is preserved under the T-shift and the SG short-range order continuously grows with a rate intrinsic to the temperature changed (cumulative memory scenario). For T-shift processes with a large ΔT the deviation from the cumulative memory scenario has been observed for the first time in the numerical simulation. We attribute the phenomenon to the 'chaos effect' which, we argue, is qualitatively different from the so-called the rejuvenation effect observed just after the T-shift.

Acknowledgements

We thank H. Yoshino for many fruitful discussions, and P.E. Jönsson, P. Nordblad, V. Dupuis, E. Vincent and H. Mamiya for discussions on their experimental results. This work is supported by a Grant-in-Aid for Scientific Research Program (# 12640369), and that for the Encouragement of Young Scientists(# 13740233) from the Ministry of Education, Science, Sports, Culture and Technology of Japan. The present simulations have been performed using the facilities at the Supercomputer Center, Institute for Solid State Physics, the University of Tokyo.

[1] E. Vincent, J. Hammann, M. Ocio, J.-P. Bouchaud and L.F. Cugliandolo: in *Proceeding of the Sitges Conference on Glassy Systems*, Ed.: E. Rubi (Springer, Berlin, 1996)

[2] J. P. Bouchau, L. F. Cugliandolo, J. Kurchan and M. Mézard: in *Spin glasses and random fields*, edited by A. P. Young, (World Scientific, Singapore, 1997).

[3] P. Nordblad and P. Svendlidh: in the same book as Ref. 2.

[4] K. Jonason, E. Vincent, J. Hammann, J.P. Bouchaud, and P. Nordblad: Phys. Rev. Lett. **81** (1998) 3243.

[5] J. P. Bouchaud: cond-mat/9910387.
[6] F. Lefloch, J.M. Hammann, M. Ocio and E. Vincent: Europhys. Lett. **18** (1992) 647.
[7] P. Doussineau, T. de Lacerda-Arôso and A. Levelut: Europhys. Lett. **46** (1999) 401.
[8] L. Bellon, S. Ciliberto and L. Laroche: Europhys. Lett. **51** (2000) 551.
[9] P.E. Jönsson, M.F. Hansen and P. Nordblad: Phys. Rev. B **61** (2000) 1261.
[10] A.J. Bray and M.A. Moore: Phys. Rev. Lett. **58** (1987) 57.
[11] D.S. Fisher and D.A. Huse: Phys. Rev. B **38** (1988) 386.
[12] D.S. Fisher and D.A. Huse: Phys. Rev. B **38** (1988) 373.
[13] T. Komori, H. Yoshino and H. Takayama: J. Phys. Soc. Jpn. **68** (1999) 3387.
[14] T. Komori, H. Yoshino and H. Takayama: J. Phys. Soc. Jpn. **69** (2000) 1192.
[15] T. Komori, H. Yoshino and H. Takayama: J. Phys. Soc. Jpn. **69** Suppl. A (2000) 355.
[16] L.W. Bernardi, H. Yoshino, K. Hukushima, H. Takayama, A. Tobo and A. Ito: Phys. Rev. Lett. **86** (2001) 720.
[17] A. Ito, A. Tobo, N. Onchi and J. Satooka: J. Phys. Soc. Jpn. **69** Suppl. A (2000) 223.
[18] P.O. Mari and I.A. Campbell: Phys. Rev. E **59** (1999) 2653.
[19] P.E. Jönsson, H. Yoshino and P. Nordblad: cond-mat/0203444.
[20] M. Picco, F. Ricci-Tersenghi and F. Ritort: Phys. Rev. B **63** (2001) 174412.
[21] L. Berthier and J.-P. Bouchaud: cond-mat/0202069
[22] J. Kisker, L. Santen, M. Schreckenberg and H. Rieger: Phys. Rev. B **53** (1996) 6418.
[23] E. Marinari, G. Parisi, F. Ricci-Tersenghi and J.J. Ruiz-Lorenzo: J. Phys. A **31** (1998) 2611.
[24] H. Yoshino, K. Hukushima and H. Takayama: cond-mat/0202110, 0203267.
[25] P.E. Jönsson, H. Yoshino, P. Nordblad, H. Aruga Katori and A. Ito: cond-mat/0112389.
[26] M. Alba, J. Hammann, M. Ocio and Ph. Refregier: J. Appl. Phys. **61** (1987) 3683.
[27] Ph. Refregier, M. Ocio, J. Hammannn and E. Vincent: J. Appl. Phys. **63** (1988) 4343.
[28] H. Mamiya, I. Nakatani and T. Furubayashi: Phys. Rev. Lett. **82** (1999) 4332.
[29] V. Dupuis and E. Vincent: private communication.
[30] H. Mamiya: private communication.
[31] V. Dupuis, E. Vencent, J.-P. Bouchaud, J. Hammann, A. Ito and H. Arga Katori: Phys. Rev. B **64** (2001) 174204.
[32] A.J. Kovacs: Adv. Poly. Sci. **3** (1963) 394; A.J. Kovacs *et al*: J. Poly. Sci. **17** (1979) 1097.
[33] P.E. Jönsson, H. Yoshino and P. Nordblad: private communication.
[34] H. Yoshino, A. Lemaître and J.-P. Bouchaud: Eur. Phys. J. **20** (2001) 174204.